ELSEVIER

Journal of Nuclear Materials 297 (2001) 1–6

journal of nuclear materials

www.elsevier.com/locate/jnucmat

# Optical phenomena in KU-1 silica core fiber waveguides under pulsed reactor irradiation

P.V. Demenkov [a], O.A. Plaksin [a,*], V.A. Stepanov [a], P.A. Stepanov [a], V.M. Chernov [a], K.M. Golant [b], A.L. Tomashuk [b]

[a] *A.I. Leypunsky Institute of Physics and Power Engineering, State Scientific Centre of Russian Federation, Kaluga region, 249033 Obninsk, Russia*

[b] *Fiber Optics Research Center, General Physics Institute of the Russian Academy of Sciences, 38 Vavilov Street, 119991 Moscow, Russia*

Received 27 October 2000; accepted 28 April 2001

**Abstract**

The light emission intensity and transient optical absorption (TOA) have been measured in the wavelength range 400–750 nm in KU-1 silica core fibers under irradiation of the BARS-6 pulsed fission reactor (pulse duration 80 μs, fluence per pulse up to $5 \times 10^{12}$ n/cm$^2$ ($E > 0.5$ eV), dose rate up to $10^5$ Gy/s). The fast light emission component attributed to Cherenkov radiation is followed by a weak emission tail with the characteristic time $(150 \pm 50)$ μs. The transient absorption reaches $2.5 \times 10^{-4}$ cm$^{-1}$ (relaxation time 600–1200 μs). The sub-linear dependence of Cherenkov radiation on the dose rate and the occurrence of both the tail of light emission and transient absorption are ascribed to the appearance of optical inhomogeneities of the silica glass under intense pulsed reactor irradiation. © 2001 Published by Elsevier Science B.V.

## 1. Introduction

The radiation sensitivity of optical fibers shows up as interference of radiation-induced luminescence (RIL), Cherenkov radiation and transient optical absorption (TOA). Numerous studies have already been performed mostly using purely ionizing irradiation (for instance, see [1,2]). However, the behavior of optical fibers in a wide variety of irradiation conditions and the mechanisms responsible for the transient optical phenomena in optical fibers under irradiation are far from being well understood.

The development and utilization of optical silica fibers in diagnostic systems of radiation facilities (especially reactors) are restrained to a great extent by both the absence of a clear theoretical view on the mechanisms of radiation-induced optical phenomena in glasses and the lack of experimental data on spectral and temporal characteristics of RIL and TOA. The review of the known results on RIL and TOA presented in the next chapter shows that these phenomena in optical silica fibers are usually attributed to the electron transitions between radiation-induced and intrinsic localized states. In spite of the electron structure of these centers being studied well enough, the problem on the mechanisms of the center formation, excitation and relaxation under intense ionizing irradiation is still open.

With this concern, experiments on light emission and optical absorption in KU-1 silica core fibers under pulsed irradiation of the BARS-6 (SSC RF IPPE) fast fission reactor have been conducted, in particular, to measure the dose rate dependence of optical properties changing with characteristic times much shorter than the reactor pulse duration (Cherenkov radiation). Experiments with the fibers of 100 m length or longer are possible in the BARS-6 reactor, which facilitates measurements of weak light emission and transient absorption. It is especially important for TOA during reactor irradiation, because most of the known data relate to

* Corresponding author. Tel.: +7-08439 98 382; fax: +7-095 230 2326.

*E-mail address:* plax@mail.ru (O.A. Plaksin).

0022-3115/01/$ - see front matter © 2001 Published by Elsevier Science B.V.
PII: S0022-3115(01)00602-X

irreversible changes of optical absorption in the fibers (magnitude higher than $10^{-3}$ cm$^{-1}$ [3]), not to the lower TOA.

## 2. Radiation-induced optical phenomena in silica glasses and fibers

According to the results of post-radiation testing [4], the fibers with a silica core of high OH-group content (600–800 ppm) can be applied in the region of 400–800 nm (transparency range) at the doses of reactor irradiation lower than $\approx 10^{17}$ n/cm$^2$. Limited use at wavelengths $>800$ nm is mainly due to the absorption bands at 950, 1250 and 1400 nm (overtones of the fundamental OH-mode of vibration responsible for absorption at 2750 and 2830 nm) [5].

In the transparency range of fibers with the high OH-group content, absorption bands at 720 and 630 nm are also observed, the first band being an overtone of the OH-mode. The second weak band at 630 nm is observed sometimes, usually ascribed [6] to the hole center associated with the non-bridging oxygen (≡Si—O). The absorption coefficient at these bands does not exceed $7 \times 10^{-4}$ cm$^{-1}$ (300 db/km) [4], which is not limiting for application of the fibers in this spectral range. However, RIL and TOA arising under irradiation may effect optical signals in the transparency ranges of fibers.

### 2.1. Radiation-induced light emission

RIL spectra of silica glasses usually include three wide bands. Under proton or $He^+$ ion irradiation (flux $\approx 5 \times 10^{14}$ ion/cm$^2$ s), bands which approximately peaked at 300, 455 and 645 nm were observed, with intensity ratios being equal to 1:60:10 (proton irradiation) or 1:40:20 ($He^+$ ion irradiation) [7].

The RIL spectra of KU-1 and KS-4V glasses during pulsed reactor irradiation (150 μs pulse, dose rate up to $3.5 \times 10^5$ Gy/s) consisted of the band at 650 nm and the tail decaying at the wavelength from ≈400 to ≈560 nm [8]. The shape of the RIL signal in the complete range of RIL observations coincided well with the shape of the excitation pulse, therefore, the characteristic lifetime of RIL was not longer than 1 μs.

In silica fibers, two wide bands of RIL were observed. Under X-ray irradiation these bands were peaked at 500 and 650 nm, the latter being weaker [9]. In [10], two RIL bands at 450 and 650 nm were observed during X-ray irradiation. The discrepancy concerning band position in [9,10] could be explained if the transient absorption interfered with RIL. Band intensities depend on temperature, dose and type of irradiation. Monotonic growth of the RIL intensity at 450 nm with the dose and RIL intensity at 650 nm independent of the dose were reported in [10].

Similar to the absorption band at 630 nm, RIL of silica glasses at 645 nm observed in [7] were attributed to the hole centers at non-bridging oxygen. The origin of the RIL band at 450 nm is probably the same as the origin of blue photoluminescence (PL). PL in the range of bands at 450 nm is excited by photons with the wavelength in the range of the absorption band of oxygen-deficient centers (≡Si—Si≡) at 248 nm. The origin of PL is equivocally ascribed to the relaxation of these centers [11]. This PL decays with time of 30 ms [11].

Sometimes, Cherenkov radiation is observed [1,3,12–14] solely or along with RIL. For example, the light emission in silica fibers under conditions of the JMTR reactor (neutron flux $\approx 10^{13}$ n/cm$^2$ s) or TFTR reactor (neutron flux $2 \times 10^{12}$ n/cm$^2$ s) was attributed to Cherenkov radiation [3,12]. The intensity of light attributed to Cherenkov radiation obeys the $\lambda^{-3}$ wavelength dependence, the characteristic decay time is shorter than some tens of nanoseconds [13].

### 2.2. Transient optical absorption

TOA was mainly examined at fixed wavelengths. TOA at 600 and 800 nm was measured in nominally pure silica core fibers (OH content not reported) under pulsed 2 MeV electron irradiation [1]. A gradual increase from $1.4 \times 10^{-3}$ cm$^{-1}$ (600 db/km) at $\approx 10^{-1}$ Gy to 1.4 cm$^{-1}$ ($6 \times 10^5$ db/km) at $\approx 10^2$ Gy was reported for TOA at 600 nm. A similar dose dependence but somewhat lower TOA at 800 nm was also observed. As in many other studies the authors of [1] did not discuss the origin of TOA.

The kinetics of TOA at 215 nm were studied in [15] on fused silica under pulsed reactor irradiation (40 ms pulse, fluence and ionizing dose per pulse $8 \times 10^{13}$ n/cm$^2$ ($E > 0.75$ MeV) and $2.5 \times 10^4$ Gy). The detected TOA pulses were characterized by the delay of 20 ms with respect to reactor pulse and the amplitude of 0.1–0.02 cm$^{-1}$, the amplitude decreasing on heating from 0°C to 500°C. The pulsed behavior of TOA and the absence of residual absorption after irradiation were explained by the radiation annealing of defects. RIL and TOA bands decaying with time of about 100 μs under pulses of 0.5 MeV electron irradiation (2 ns pulse) were observed in [16].

## 3. Experimental

The schematic diagram of the measurements of radiation-induced optical properties of optical fibers under pulsed irradiation of the BARS-6 fission reactor (pulse duration 80 μs, fluence per pulse $\leqslant 5 \times 10^{12}$ n/cm$^2$ ($E > 0.5$ eV), dose rate $\leqslant 10^5$ Gy/s) is given in Fig. 1. The registration and data acquisition system included PMT with the pre-amplifier and multichannel ADC

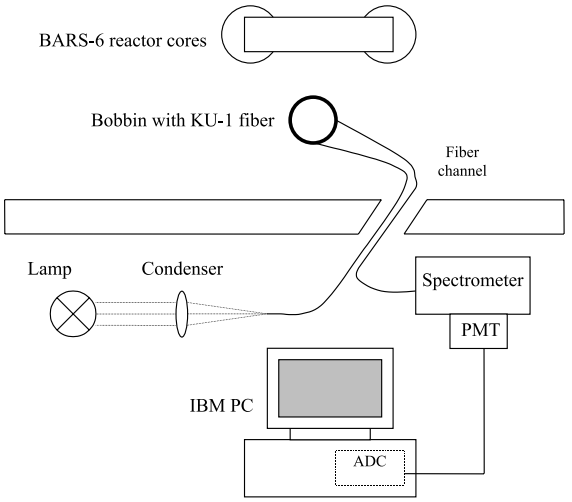


Fig. 1. Schematic diagram of the radiation-induced optical effects experiment.

placed in the PC. The system provides a means of measurement with a resolution time down to 100 ns in the spectral range 400–800 nm.

Two optical fiber samples of the KU-1 silica core (OH content 1000 ppm), fluorine-doped cladding and polymer coating with core diameters of 100 μm and 1 mm were wound on aluminum bobbins (length 20 and 10 m, respectively) and placed near active cores of the BARS-6 reactor. The optical fibers (cladding thickness 10 μm, numerical aperture 0.16) were produced by FORC GFI RAS using a technique of outside deposition of fluorine-doped silica glass in a microwave plasma torch [17]. The initial optical absorption coefficient (Fig. 2) in the range 400–800 nm was not higher than $1.1 \times 10^{-4}$ cm$^{-1}$.

The optical signals and the neutron flux were measured simultaneously in our experiments. The neutron pulse was registered by means of an evacuated fission

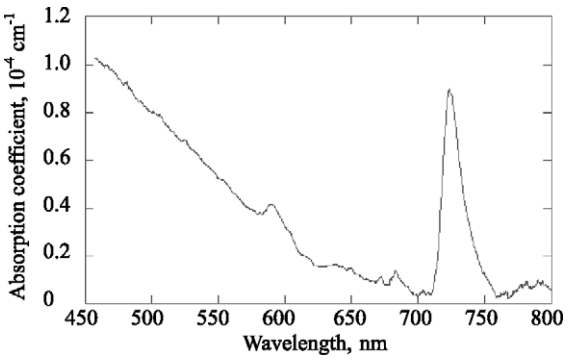


Fig. 2. Initial absorption spectrum of the KU-1 fiber of 100 μm core diameter.

chamber placed in a boron-containing case (for counting neutrons with $E > 0.5$ eV) as well as a self-switching amplifier, ADC and PC. The dose per pulse was determined from the residual activity of nickel samples. The absorbed dose was calculated with the help of the MCNP code [18] taking into account the energy transfer due to gamma irradiation, the collisions involving neutrons and neutron absorption.

In processing the optical signal passing through a fiber, it is necessary to separate contributions from light emission and TOA. Assuming $Q$ to be the light emission power per unit volume, $L$ the fiber length under irradiation, $D = \alpha L$ the optical density of the fiber ($\alpha$ is the absorption coefficient), $NA$ the numerical aperture, $n$ the refraction index of silica glass, the intensity of the light caused by light emission coupling out the fiber is given by the expression

$$I_1 = \frac{QL(1 - \exp(-D))}{D} \frac{NA^2}{2n^2}, \tag{1}$$

where a portion of the isotropic light emission is considered to be lost outside the aperture angle defined by $\sin(\theta) = NA/n$.

Eq. (1) shows a strong dependence of the light-emission signal on TOA. But in many studies on RIL, the effect of TOA was not taken into account. For instance, because of the difference in temperature and dose dependence, the RIL bands at 500 and 650 nm in [9] were concluded to be of different origins. Obviously, without data on TOA at 500 and 650 nm similar conclusions are not well grounded.

Light emission, in its turn, interferes with the light signal transmitting through a fiber. The light (intensity $I_0$) coupled to the fiber weakens due to TOA and is added to emitted light. The optical signal from the fiber under irradiation and simultaneous probing with light is given by the expression

$$I_2 = I_1 + I_0 \exp(-D), \tag{2}$$

where $I_1$ is given by Eq. (1). After measurement of $I_1$ and $I_2$ one can calculate the optical density $D$ and power of light emission $Q$ from Eqs. (1) and (2)

$$D = \ln\left(\frac{I_0}{I_2 - I_1}\right), \tag{3}$$

$$QL\frac{NA^2}{2n^2} = \frac{I_0 I_1 D}{I_0 + I_1 - I_2}. \tag{4}$$

To separate light emission and TOA the intensity of light emission in the fibers or the intensity of simultaneous light emission and probing light (filament lamp or lasers) were measured.

## 4. Results

Fig. 3 represents the optical signals registered in the range of well-known absorption bands at ≈630 nm. This band, however, was not observed in the initial spectra. Due to interference between light emission and absorption the pulse of light emission is not observed during the measurement with probing light. The time dependences of the emission power and optical density $D$ calculated by use of Eqs. (3) and (4) are shown in Fig. 4. TOA reaches $3.5 \times 10^{-4}$ cm$^{-1}$ (160 db/km) in its maximum. This absorption is two times larger than the initial absorption and corresponds to an efficiency of $3.5 \times 10^{-9}$ cm$^{-1}$/Gy s. For instance, in experiments with fused silica [15], the ionizing efficiency of TOA at 215 nm reached $1.5 \times 10^{-8}$ cm$^{-1}$ Gy$^{-1}$ s at the leading edge of reactor pulses.

Two stages of TOA decay with characteristic times of about 130 μs and 600–1200 μs are observed. The TOA maximum is observed later than ≈20 μs after the maximum of the neutron pulse (Fig. 4). Backward TOA at 215 nm was also observed in the study [15] during pulsed reactor irradiation of fused silica. The pulse of TOA and the absence of residual absorption after the irradiation were explained by radiation annealing of defects. However, this explanation is not satisfactory for TOA decaying with times of 600–1200 μs much exceeding the pulse duration.

In the range of well-known RIL bands at 450 nm the TOA does not exceed $1 \times 10^{-4}$ cm$^{-1}$ (45 db/km) up to a dose of $10^2$ Gy, neither delay nor slow decay being observed. No residual absorption in the range 400–800 nm was observed after irradiation to a dose of $10^3$ Gy.

The time dependence of light emission (Figs. 4 and 5) has a fast component, whose maximum is at the same time as the maximum of the neutron pulse (maximum intensity of gamma radiation accompanying a neutron pulse). After the fast component, later than 50 μs after the maximum of the neutron pulse, a tail of light emission is observed (slow component), which in this study is ascribed to RIL. The efficiency of conversion of absorbed ionizing energy into light emission is rather low, it does not exceed $10^{-8}$ nm$^{-1}$. In the range 400–750 nm the integrated efficiency of the conversion is of about $10^{-6}$.

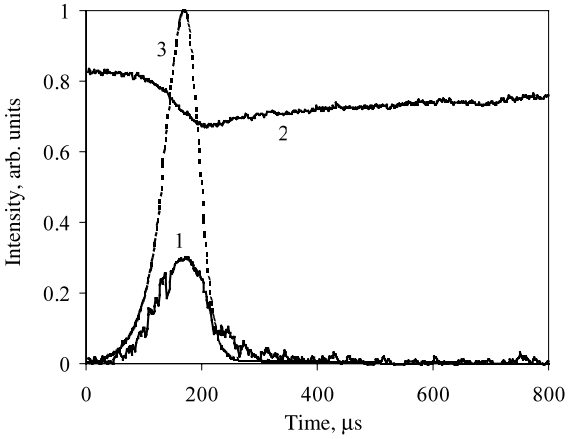


Fig. 3. Time dependence of the optical signals from the KU-1 fiber of 100 μm core diameter at the wavelength of 632 nm: without probing (1) and with probing light (2). Curve (3) – neutron flux. All values are given in arbitrary units.

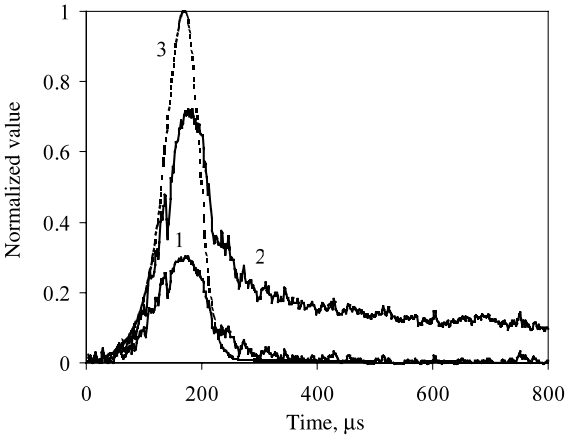


Fig. 4. Calculated time dependence: (1) normalized light emission power per unit volume ($QLNA^2/2I_0n^2$) in the KU-1 fiber of 100 μm core diameter at 632 nm; (2) optical density $D$; (3) neutron flux normalized to unity.

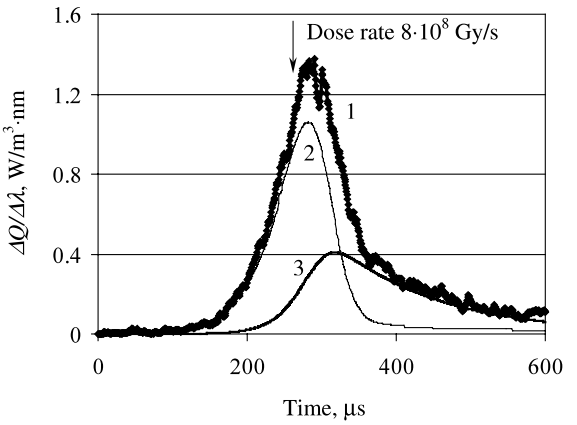


Fig. 5. Time dependence of the spectral power of light emission per unit volume ($\Delta Q/\Delta\lambda$) at 450 nm in the KU-1 fiber of 1 mm diameter: (1) experimental values; (2) power dependence of light intensity on the neutron flux with the exponent equal to 0.67 (fast component $I_{\text{fast}}(t)$); (3) dependence of light intensity corresponding to Eq. (5) with $\tau = 130$ μs (slow component $I_{\text{RIL}}(t)$).

In our experiments, the ionizing component of irradiation resulting in light emission is characterized by a dose rate proportional to the neutron flux $F(t)$, according to calculations by use of the MCNP code [18]. Fig. 5 represents the result of fitting the experimental time dependence of light emission $I(t)$ in the fiber of 1 mm diameter with the sum $(I_{\text{fast}}(t) + I_{\text{RIL}}(t))$ of a power dependence on the neutron flux (fast component $I_{\text{fast}}(t)$) and the following dependence:

$$I_{\text{RIL}}(t) \sim \int_0^t \left(F(t')\mathrm{e}^{(t'-t)/\tau}\right) \mathrm{d}t', \tag{5}$$

where the relaxation behavior of RIL (characteristic time $\tau$) is considered. In Eq. (5) the contributions of electronic excitation at the previous moments $t'$ into the RIL at the moment $t$ are taken into account. The rate of RIL excitation is assumed to be proportional to the ionizing dose rate, that is, proportional to the neutron flux.

Probably, the fast component is of Cherenkov origin. The spectral intensity of this component at a constant ionizing dose rate decreases with increasing wavelength ($\lambda$) as a function of $1/\lambda^3$ (Fig. 6). However, this intensity is not proportional to the dose rate as expected for Cherenkov radiation, it obeys a power dependence with the exponent of $0.70 \pm 0.05$. The sub-linear dependence is not caused by optical absorption, since the dependence is found after separation of light emission and TOA (Fig. 4). This non-linearity is probably caused by the increasing inhomogeneity of glass with increasing dose rate, probably due to collision cascades, where electric charge partitioning and thermal spikes occur. As pointed out in [19], the Cherenkov radiation yield decreases with increasing inhomogeneity. Simultaneously, due to scattering in inhomogeneous glass the decrease of the optical transmission of the fiber may occur, which is probably observed in pulsed TOA in the regions of transparency.

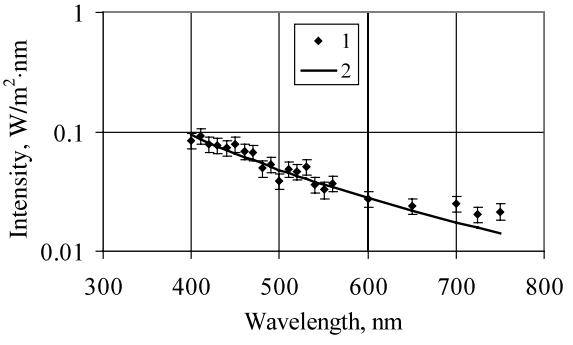


Fig. 6. Spectral intensity (per unit area) of: (1) light emission $I$ at the outlet of the KU-1 fiber of 1 mm diameter at the ionizing dose rate of $8 \times 10^4$ Gy/s (see arrow in Fig. 4) and (2) the shape of a spectrum of Cherenkov radiation.

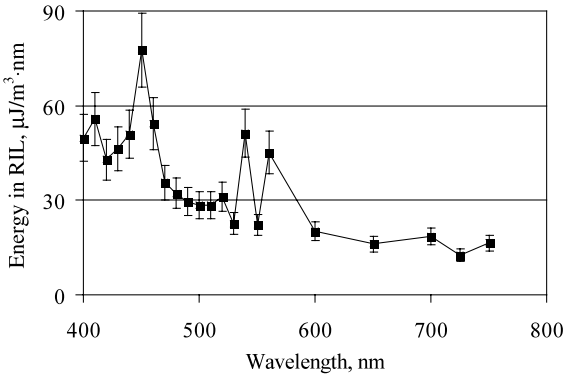


Fig. 7. Spectrum of the slow component (spectral power of light emission per unit volume ($Q/\Delta\lambda$) integrated over time) for the KU-1 fiber of 1 mm diameter. The integration is aimed to reduce the effect of errors of calculation.

The characteristic decay time of RIL (Fig. 5) is about $(150 \pm 50)$ μs (compared to the TOA decay time of 130 μs) and does not change with the dose up to $\approx 10^3$ Gy. The time of 100 μs corresponds to the characteristic decay time of RIL and TOA in silica fibers after pulses of 0.5 MeV electron irradiation (2 ns pulse) observed in [16]. Probably, RIL and TOA are related through charge carrier recombination.

The origin of the slow component of light emission (RIL) is not known. In the RIL spectrum (Fig. 7), the band at 450 nm and the band in the region of 530–560 nm are probably observed against the background of the general decrease of the RIL intensity with increasing wavelength. However, RIL is not due to relaxation of oxygen deficient centers, whose characteristic time is much longer (≈30 ms) [11]. Since the relaxation component with approximately the same characteristic time is observed in the complete region of 400–750 nm, this time probably does not characterize RIL centers. This time can be attributed to charge transfer to RIL centers.

## 5. Conclusion

Measurements of the light emission intensity and TOA at 400–700 nm in KU-1 silica glass core fiber waveguides under irradiation of the BARS-6 pulsed fission reactor (80 μs pulse, fluence per pulse up to $5 \times 10^{12}$ n/cm$^2$ ($E > 0.5$ eV), dose rate up to $10^5$ Gy/s) have shown that Cherenkov radiation is the strongest radiation-induced optical effect in silica core fibers at least up to a dose of $10^3$ Gy. The sub-linear dose rate dependence of the Cherenkov radiation intensity (power of $0.70 \pm 0.05$) indicates probably the appearance of optical inhomogeneity in the core of the fiber during neutron pulses.

RIL and TOA are weaker effects up to a dose of $10^3$ Gy. The technique used in the present study for measurements and data processing is suitable to determine RIL and TOA. The latter reaches $2.5 \times 10^{-4}$ cm$^{-1}$ (110 db/km) in the range where the absorption band at 630 nm is often observed before or after irradiation in other studies. It appears difficult to attribute the RIL and TOA to any definite optical centers in the glass. TOA is probably apparent and is caused by the light scattering due to optical inhomogeneity arising under irradiation. The weak dependence of the characteristic time of RIL on the wavelength indicates a relationship of this time with the charge transfer in the glass.

## Acknowledgements

The study was supported by Russian Foundation for Basic Research (Grants No. 98-02-03571 and 99-02-16856).

## References

[1] J.E. Golob, P.B. Lyons, L.D. Looney, IEEE Trans. Nucl. Sci. 24 (1977) 2154.
[2] P.L. Mattern, L.M. Watkins, C.D. Skoog, J.R. Brandon, E.H. Barsis, IEEE Trans. Nucl. Sci. 21 (1974) 81.
[3] T. Shikama, T. Kakuta, M. Narui, T. Sagava, N. Shamoto, T. Uramoto, K. Sanada, H. Kayano, J. Nucl. Mater. 212–215 (1994) 421.
[4] D.W. Cooke, E.H. Farnum, B.L. Bennett, in: Fusion Materials Semiannual Progress Report for the Period Ending, DOE/ER-0313/20, Oak Ridge National Laboratory, 1996, p. 275.
[5] E.J. Friebele, D.L. Griscom, J.J. Marrone, J. Non-Cryst. Solids 71 (1985) 133.
[6] D.L. Griscom, J. Ceram. Soc. Jpn. 99 (1991) 923.
[7] O.V. Kalantaryan, S.I. Kononenko, V.I. Muratov, in: V.F. Zelensky (Ed.), Proceedings of the International Conference on Radiation Material Science, Alushta-1990, vol. 9, Kharkov Institute of Physics and Chemistry, 1991, p. 142 (in Russian).
[8] A. Gorshkov, D. Orlinsky, V. Sannikov, V. Vukolov, S. Goncharov, Yu. Sadovnikov, A. Kirillov, J. Nucl. Mater. 273 (1999) 271.
[9] D.W. Cooke, B.L. Bennett, E.H. Farnum, A.M. Portis, M.S. Jahan, D.E. Thomas, ITER Workshop at ICFRM-7, Obninsk, 1995.
[10] M.J. Marrone, Appl. Phys. Lett. 38 (1981) 115.
[11] R. Tohmon, Y. Shimogaichi, H. Mizuno, Y. Ohki, K. Nagasawa, Y. Hama, Phys. Rev. Lett. 62 (1989) 1388.
[12] S.F. Paul, J.L. Goldstein, R.D. Durst, R.J. Fonck, Rev. Sci. Instrum. 66 (1995) 1252.
[13] W. Schneider, U. Babst, Proc. SPIE 506 (1984) 189.
[14] F. Sato, Y. Oyama, T. Iida, F. Maekava, J. Datemichi, A. Takahashi, Y. Ikeda, in: Proceedings of the 19th Symposium on Fusion Technol., 1996, p. 857.
[15] G.E. Palma, R.M. Gagosz, J. Phys. Chem. Solids 33 (1972) 177.
[16] D.L. Griscom, in: Proceedings of the 33rd Frequency Control Symposium, Electronics Industries Association, Wasington, DC, 1979, p. 98.
[17] A.S. Biriukov, E.M. Dianov, K.M. Golant, R.R. Khrapko, A.V. Koropov, A.N. Perov, A.V. Shakhanov, S.A. Vasiliev, Sov. Lightwave Commun. 3 (1993) 1 (in Russian).
[18] J.F. Briesmeister (Ed.), MCNP – a General Monte Carlo Code for Neutron and Photon Transport, LANL LA-7396, Rev. 2, 1986.
[19] M.I. Ryazanov, Electrodynamics of Condensed Matter, Nauka, Moscow, 1984 (in Russian).